1
2
3

Yorkie is required to restrict the injury responses in planarians

Alexander Y.T. Lin[1,2] and Bret J. Pearson[1,2,3]*

[1] *Hospital for Sick Children, Program in Developmental and Stem Cell Biology;*
[2] *Department of Molecular Genetics, University of Toronto;*
[3] *Ontario Institute for Cancer Research;*
Toronto, ON, M5G10A4, CANADA

Running title: Yorkie regulates the wound program in planarians

*Correspondence should be addressed to: Bret Pearson (email: bret.pearson@sickkids.ca)

20   **Abstract**

21

22   Regeneration requires the precise integration of cues that initiate proliferation, direct

23   differentiation, and ultimately re-pattern tissues to the proper size and scale. Yet how these

24   processes are integrated with wounding cues remains relatively unknown. The freshwater

25   planarian, *Schmidtea mediterranea,* is an ideal model to study the stereotyped proliferative and

26   transcriptional responses to injury due to its high capacity for regeneration. Here, we characterize

27   the effector of the Hippo signalling cascade, *yorkie*, during planarian regeneration and its role in

28   restricting early injury responses. In *yki(RNAi)* regenerating animals, wound responses are hyper-

29   activated; the bimodal proliferation kinetics are heighted and prolonged, while the transcriptional

30   injury responses are similarly augmented with dysregulated temporal patterns. We also

31   uncovered novel wound-induced genes by RNAseq that are primarily associated with tissue

32   patterning. Indeed, a high proportion of non-wound- and wound-induced patterning molecules

33   are mis-expressed in *yki(RNAi)*, which we demonstrate is in part due to an expanded muscle cell

34   population. These altered injury responses have consequential effects on regenerative outcomes,

35   specifically sensing the size of a given injury and appropriately scaling organ and tissue sizes.

36   Taken together, our results suggest that *yki* functions as a key node to integrate the injury

37   responses of proliferation, apoptosis, injury-induced transcription, and patterning to coordinate

38   regeneration.

39

Introduction

Regeneration is a growth-controlled program that is observed across the animal kingdom. Neo-natal mice can regrow missing digit tips, salamanders can replace missing limbs, while other organisms, such as hydrazoans and planarians, can regenerate virtually any tissue (Holstein et al., 2003; Rinkevich et al., 2011; Sanchez Alvarado, 2000; Takeo et al., 2013; Thornton, 1968). The shared characteristic to regenerate suggests a conserved genetic program that first replaces the missing tissue by proliferation (epimorphosis) and subsequently re-patterns and re-scales (morphallaxis) the regenerated tissue (Morgan, 1898; Morgan, 1901). Failure to initiate or cease aspects of either process can result in under- or overgrown tissues, respectively. Yet how proliferation and patterning are regulated in the correct spatiotemporal manner to determine size and scaling of regenerating tissues remains poorly understood.

The asexual planarian, *Schmidtea mediterranea*, displays a remarkable ability control growth because it can regenerate any missing tissue upon amputation, then rescale the entire animal in proportion to the remaining tissue. Planarian regenerative capacity is derived from its near ubiquitous population of adult stem cells (neoblasts), which are also the only mitotic cells in the animal and at least some of which are pluripotent (Reddien and Alvarado, 2004; Saló and Baguna, 1989; Wagner et al., 2011). In response to tissue removal, a stereotypical bimodal pattern of proliferation occurs first at 6 hours post amputation (hpa) and then at 48 hpa (Wenemoser and Reddien, 2010). Moreover, a common transcriptional injury response program is expressed with distinct temporal and spatial patterns (Wenemoser et al., 2012; Wurtzel et al., 2015). However, it is unknown how these two processes may be linked and what regulators may determine the onset or decay of these responses. As regeneration progresses, the missing tissues are replaced, reintegrated with the prexisiting tissue, and finally rescaled to restore tissue sizes

63   and proportion. This rescaling process, also known as morphallaxis, is crucial to achieve proper

64   proportions of the regenerated animal (Morgan, 1898; Morgan, 1901). For example, in planarians

65   the WNT polarity gradients must be rescaled to accommodate the new size of the worm (Gurley

66   et al., 2010). Therefore, the planarian is a unique model to understand the dynamic processes of

67   growth—proliferation, patterning, and scaling—in an adult regenerative context.

68   The Hippo pathway is universal regulator of growth control and is a kinase cascade that

69   impinges on the transcriptional co-activator, Yorkie, (in vertebrates: YAP1/2 and paralog TAZ)

70   (Halder and Johnson, 2011; Huang et al., 2005). Constitutive activation of Yki or YAP results in

71   overgrown tissues in flies and vertebrates, suggesting a conserved role in promoting cell division

72   (Camargo et al., 2007; Dong et al., 2007; Huang et al., 2005). However, YAP can be growth-

73   restrictive in highly proliferative and regenerative tissues, such as the mammalian intestine

74   (Barry et al., 2012). Indeed, we have previously demonstrated that planarian *yorkie/YAP* (*Smed-*

75   *yki*) is required to restrict stem cell proliferation, yet *yki(RNAi)* animals failed to regenerate (Lin

76   and Pearson, 2014). This conundrum between increased proliferation with an undergrowth

77   phenotype suggests other intricacies of growth control are dysregulated, but this remains to be

78   tested. Here, we demonstrate that Yki is required for the regeneration of appropriately scaled

79   and sized tissues by integrating the wound signals that direct the proliferative, apoptotic, and

80   transcriptional injury responses. In *yki(RNAi)* animals, these known injury responses are hyper-

81   activated with dysregulated patterns. Indeed, the proliferative dynamics are heighted and

82   temporally prolonged. This enlarged stem cell population showed no block in differentiation, and

83   surprisingly, showed increased numbers of both epidermal and *collagen*^{+} muscle cells. The

84   expansion of these cell types can be attributed to a subsequent heighted transcriptional injury

85   response. Using an RNA-deep sequencing (RNAseq) time course, we determined that *yki(RNAi)*

86   regenerates had significantly dysregulated wound-induced genes, which have predominant roles

87   in patterning. Thus, with altered proliferation kinetics and dysregulated expression of patterning

88   molecules, *yki(RNAi)* animals failed to maintain proper size and scaling during morphallaxis.

89   Altogether, this study demonstrates that the injury responses of proliferation and transcription are

90   required to set up proper regenerative outcomes, such that *yki* is the crucial node that integrates

91   these processes.

92

93   **Methods**

94   *Animal husbandry, Exposure to γ-Irradiation, and RNAi*

95   Asexual *Schmidtea mediterranea* CIW4 strain were reared as previously described (Sánchez

96   Alvarado, 2002). For irradiation experiments, planarians were exposed to 60 Gray (Gy) of γ-

97   irradiation from a ^{137}Cs source (Pearson and Sánchez Alvarado, 2010). RNAi experiments were

98   performed using previously described expression constructs and HT115 bacteria (Newmark et

99   al., 2003). Bacteria were grown to an O.D.600 of 0.8 and induced with 1 mM IPTG for 2 hours.

100   Bacteria were pelleted, mixed with liver paste at a ratio of 500 µl of liver to 100 ml of original

101   culture volume, and frozen as aliquots. The negative control, "*control(RNAi)*", was the *gfp*

102   sequence as previously described (Cowles et al., 2013). All RNAi food was fed to one week

103   starved experimental worms every 3rd day for a total of 3 feedings. Amputations were performed

104   15 days after the final feeding with corresponding salt addition to suppress the homeostatic

105   edema phenotype (Lin and Pearson, 2014). All animals were size-matched between experimental

106   and control worms.

107

108   *Pharynx Amputations*

109   Pharynxes were chemically amputated by replacing planarian water with 100 mM sodium azide

110   (NaN$_3$) diluted in planarian water. After 7-10 minutes of gentle swirling and pipetting, pharynxes

111   were either entirely extruded or extended, which required forceps for complete removal. NaN$_3$

112   was vigorously washed out with planarian media and subsequently fixed (Adler et al., 2014;

113   Pellettieri et al., 2010).

114

115   *CHX experiments*

116   Cycloheximide (Sigma) was added immediately to animals following amputation as previously

117   described (Wenemoser et al., 2012).

118

119   *Quantitative Real-Time PCR (qRT-PCR)*

120   Reverse transcription reactions were conducted on total RNA extracted from approximately 15

121   worms using a SuperScript III Reverse Transcriptase Kit (Invitrogen). Quantitative real-time

122   PCR was performed in biological triplicate on a Bio-Rad CFX96 Touch™ Real-Tie PCR

123   Detection System with SYBR Green PCR Master Mix (Roche) as per manufacturer's

124   instructions. The $2^{-\Delta\Delta CT}$ method was used for relative quantification. Primer pairs for

125   ubiquitously expressed GAPDH were used as a reference as previously described (Eisenhoffer et

126   al., 2008a) and regeneration time courses experiments were normalized to *control(RNAi)* intact

127   levels.

128

129   *Immunolabeling, BrdU, TUNEL, and in situ hybridizations (ISH)*

130   Whole-mount ISH (WISH), and double fluorescent ISH (dFISH), and immunostainings were

131   performed as previously described (Currie et al., 2016a; Lauter et al., 2011; Pearson et al., 2009).

132   Colorimetric WISH stains were imaged on a Leica M165 fluorescent dissecting microscope.

133   dFISH and fluorescent phospho-histone H3 (rabbit monoclonal to H3ser10p, 1:500, Millipore)

134   immunostains were imaged on a Leica DMIRE2 inverted fluorescence microscope with a

135   Hamamatsu Back-Thinned EM-CCD camera and spinning disc confocal scan head. BrdU (Sigma

136   B5002-5G, 25 mg/ml) was dissolved in 50 % ethanol and fed to animals and was stained as

137   previously described (Zhu et al., 2015). TUNEL was performed as previous described (Pellettieri

138   et al., 2010) with the Terminal Deoxynucleotidyl Transferase enzyme (Thermo, EP0162). Cell

139   counts and co-localizations were quantified using freely available ImageJ software

140   (http://rsb.info.nih.gov/ij/). Significance was determined by a 2-tailed unequal variance pairwise

141   student's *t*-test. All images were post-processed in a similar manner using Adobe Photoshop.

142

143   *RNA sequencing and Differential Expression Analysis*

144   RNA deep sequencing (RNAseq) was performed on 1 day post-irradiated animals with no

145   amputation (intact) or tail fragments regenerating at 6, 12, and 24 hours post amputation.

146   Experiments were performed in biological-triplicate, sequenced to a depth of >20 million reads

147   per sample, and multiplexed on an Illumina HiSeq2500 with 50 base pair, single-end reads. Raw

148   scRNAseq data from uninjured cells (including stem cells, neurons, gut, epithelial, muscle and

149   peripharyngeal cells) were obtained from the NCBI Sequence Read Archive

150   (SRA:PRJNA276084) (Wurtzel et al., 2015). Reads were aligned to the SmedASXL

151   transcriptome assembly under NCBI BioProject PRJNA215411 using bowtie2 (Langmead and

152   Salzberg, 2012) with 15 bp 3' trimming. For validating and detecting novel wound-induced

153   genes, DEseq2 was used for differential expression analysis on triplicated regenerating samples

154   at each time point compared to intact animals (Love et al., 2014). The parameters for

155   significance calling were [FC] (fold change) > 1.2 with a [FDR] (false discovery rate) < 0.05. To

156   detect mis-expressed patterning molecules, DEseq2 was run on the triplicated *yki(RNAi)* samples

157   and the matched *control(RNAi)* with [FC] > 1.2 or [FC] <0 .83 with a [FDR] < 0.05. Violin plots

158   were produced using modified source code from (Macosko et al., 2015) and heatmaps were

159   produced using the modified heatmap.3 source code from (Molinaro and Pearson, 2016).

160

161   **Results**

162   *yorkie regulates stem cell proliferation during regeneration*

163   We previously reported that *yki* is required for planarian regeneration, but the underlying

164   cause remained to be elucidated. Over 90% of *yki(RNAi)* tail fragments showed no evidence of a

165   blastema at 5 days post-amputation (dpa) and failed to regenerate, while head and trunk

166   fragments failed to a lesser degree (Lin and Pearson, 2014). Because tail fragments were the

167   most severely affected, we chose to focus our characterization on tails.

168   Failures in regeneration are often correlated with aberrant stem cell dynamics, including

169   stem cell proliferation. Thus, we first examined proliferation with mitotic marker phosphorylated

170   histone 3 (H3P). In a *control(RNAi)* regeneration time course, proliferation occurred in a bimodal

171   pattern with two bursts of proliferation that occurred at 6 and 48 hours post amputation (hpa), as

172   previously described (Figure 1A) (Wenemoser and Reddien, 2010). However, in *yki(RNAi)*

173   animals, this bimodal pattern was perturbed temporally and in its amplitude. The first wave of

174   proliferation was prolonged and peaked 15 hours later at 24 hpa. The onset of second wave of

175   proliferation was delayed and peaked at 72 hpa in *yki(RNAi)* animals (Figure 1B). Therefore, *yki*

176   was required to restrict the proliferation response to injury, which was also observed in head and

177   trunks (Supplemental Figure 1A-D).

178   Canonical target genes for *Drosophila* Yki are cell cycle regulator *cyclin E* and apoptosis

179   inhibitor *diap1* (Huang et al., 2005). Thus, the increased proliferation in *yki(RNAi)* could be

180   attributed to a change in the cell cycle. Using BrdU pulse-time-chase experiments, we examined

181   the proportion of label retaining cells at the wound margin (Figure 1C). The quantification of S-

182   phase (BrdU$^+$) or G2/M-phase (H3P$^+$) cells suggested that *yki* does not inhibit the entry or exit

183   into S-phase. Moreover, the ratio of label retaining cells (H3P$^+$/*piwi-1*$^+$/BrdU$^+$) to the total

184   amount of H3P cells was not different between *control(RNAi)* and *yki(RNAi)*, 59±9% and

185   60±7%, respectively, despite higher proliferation in *yki(RNAi)* (Figure 1D). If *yki* affected the

186   cell cycle, a difference in the percentages would be expected, however, the opposite was seen.

187   Therefore, the changes in proliferation in *yki(RNAi)* animals cannot be attributed to alterations in

188   the length of the S or G2 phase individually, although we cannot rule out the possibility that the

189   whole cell cycle is accelerated. Finally, the increased proliferation did not change stem cell

190   subclass identities (Figure 1E) (van Wolfswinkel et al., 2014) and proliferating cells were also

191   not undergoing apoptosis because no H3P$^+$/TUNEL$^+$ cells were observed (Supplemental Figure

192   1E-F).

193   In response to amputation, a wave-like pattern of proliferation emanates from the wound

194   site over time, suggesting a diffusion-based mechanism that triggers proliferation (Elliott and

195   Alvarado, 2013; Wenemoser and Reddien, 2010). For instance, proliferation predominantly

196   occurs at the wound margin at 48 hpa and subsequently shifts posteriorly by 72 hpa (Figure 1F).

197   However, in *yki(RNAi)*, proliferation was sustained at the wound margin at 72 hpa (Figure 1F).

198   This suggested the possibility of a cell non-autonomous proliferative cue that is upregulated in

199   *yki(RNAi)*. Indeed, we have previously reported that *yki* was not enriched in the stem or

200   progenitor cell populations by bulk RNA sequencing (Lin and Pearson, 2014). Congruent with

201   our previous results, single cell RNA sequencing (scRNAseq) of stem and differentiated tissues

202   also demonstrated that *yki* was not enriched in any of the stem cell sub-classes (γ, ζ or σ), and

203   instead, is primarily expressed in differentiated tissues, such as the epidermis, muscle, and gut

204   (Figure 1G). Interestingly, these same differentiated tissues have recently been shown to be

205   enriched for the expression of wound-induced genes, collectively known as the transcriptional

206   injury response (Wurtzel et al., 2015). Therefore, we next tested whether defects in the early

207   transcriptional response to wounds could explain defects observed in *yki(RNAi)* regenerates.

208

209   *yki is required to restrict the transcriptional injury response*

210   In planarians, the transcriptional wounding response program is activated immediately

211   following any type of injury, whether tissue is removed—such as a wedge cut and an

212   amputation—or not, like an incision and a poke (Wenemoser et al., 2012). This response can be

213   subcategorized temporally into two waves of transcription, an early immediate wave that peaks

214   in expression by 6 hpa, and a subsequent late sustained wave that prolongs in expression until 24

215   hpa (Wenemoser et al., 2012; Wurtzel et al., 2015). In *yki(RNA), fos-1*, an early wave marker,

216   was precociously expressed earlier at 0.5 hpa and was prolonged until 12 hpa (Figure 2A).

217   Likewise, the late marker *delta-1* was also increased and temporally unrestricted in its expression

218   (Figure 2B). The time courses observed by WISH were supported by parallel experiments using

219   qRT-PCR (Figure 2C-D). Two other wound-induced genes, *jun-1* and *tyrosine-kinase2*, showed

220   similar, upregulated expression in regenerating *yki(RNAi)* head, trunk, and tail fragments

221   (Supplemental Figure 2A-B). Additionally, irradiated animals showed no difference in *fos-1* or

222   *delta-1* expression compared to their non-irradiated controls, suggesting that the increased

223   mitoses in *yki(RNAi)* did not contribute to the elevated wound-induced gene expression (Figure

224   2E-G). Furthermore, *yki* itself was not injury-induced (Supplemental Figure 2C) and

225   cycloheximde, which blocks protein translation, did not alter the transcriptional response

226   (Supplemental Figure 2D-E) (Wenemoser et al., 2012). Finally, edemas did not affect the

227   proliferative or transcriptional injury responses, demonstrating that the pleiotropic effects of *yki*

228   on the excretory system were independent (Supplemental Figure 3) (Lin and Pearson, 2014). Due

229   to the specificity of dysregulated wound-response transcripts in *yki(RNAi)* fragments, we next

230   tested whether this could be used to discover novel wound-induced programs.

231

232   *The identification of novel wound-induced genes by RNAseq*

233   The loss of restriction in the transcriptional injury response in *yki(RNAi)* suggested that

234   transcriptome profiling *yki(RNAi)* animals may uncover novel wound-induced genes. Previous

235   studies have focused on isolating and sequencing small wound pieces instead of the whole

236   amputated fragment. Although this approach has been very successful (Wenemoser et al., 2012;

237   Wurtzel et al., 2015), it would removes candidates whose expression may be induced away from

238   the wound site. Moreover, we chose to irradiate animals because *yki(RNAi)* caused an expanded

239   stem cell population, which could greatly alter many non-injury response transcripts (Figure 1A-

240   B) (Lin and Pearson, 2014). Therefore, we conducted RNA-deep sequencing (RNAseq) on 1 day

241   post-irradiated intact animals as well as regenerating tails at 6, 12, and 24 hpa.

242   First, we conducted validation on a set of 128 previously identified wound-induced genes

243   (Wurtzel et al., 2015). We curated this list to 97 transcripts for our analyses, removing stem cell

244   enriched transcripts because our samples were irradiated. By pair-wise DEseq2 comparison of

245   *yki(RNAi)* to the respective *control(RNAi)* time point, we identified 32 of the 97 (33%)

246   transcripts significantly upregulated (fold change [FC] > 1.2, false discovery rate [FDR] < 0.05)

247   at any time point (Supplemental Table 1). By normalizing the expression to *control(RNAi)*

248 intacts, an elevated response was evidently observed in *yki(RNAi)* tail fragments (Figure 2H).

249 Consistent with the above WISH and qRT-PCR data, *jun-1, delta-1*, and *fos-1* were also

250 significantly upregulated by these analyses (Figure 2H). We further validated the upregulation in

251 *yki(RNAi)* with another *bona fide* injury marker that we had not previously examined, *Smed-sp5,*

252 which is a downstream target of *Smed-β-catenin* that is also wound-induced (Reuter et al., 2014;

253 Wurtzel et al., 2015). We observed that *Smed-sp5* was precociously expressed in *yki(RNAi)*

254 animals at 6 hpa and was sustained well beyond its normal temporal peak (Supplemental Figure

255 4A).

256   In order to find novel wound-induced genes, we used DEseq2 to compare RNAseq from

257 *control(RNAi)* intact worms to 6, 12, and 24 hpa tail fragments. This analysis generated a list of

258 341 significantly upregulated transcripts ([FC] > 2, FDR < 0.05). Using this list, we compared

259 *yki(RNAi)* to *control(RNAi)* regenerates at their matched time points ([FC] > 1.25, FDR < 0.05),

260 which resulted in a list of 42 transcripts, only 9 of which have been previously characterized.

261 Interestingly, multiple patterning molecules were identified, including HOX proteins *Smed-Post-*

262 *2c, -2d, Hox4b, Hox7c*, and WNT-signalling pathway genes *wnt-11-1, -11-2,* and *Frz-4-2* (Figure

263 2I) (Supplemental Table 2). *Smed-Post-2d*, which is similar to an AbdominalB-like homeobox

264 protein, was wound-induced with expression that peaked at 12 hpa (Figure 2J) (Currie et al.,

265 2016a; Iglesias et al., 2008). By contrast, in *yki(RNAi)*, the response was induced earlier,

266 heighted, and sustained (Figure 2J). Moreover, this trend was also observed for *IMDH2* (Figure

267 2K) and *beta-catenin-like* (Supplemental Figure 4B). Interestingly, by scRNAseq analyses, all 3

268 novel candidates had expression in the muscle, while *Smed-Post-2d* and IMDH2 also had

269 predominant enrichment in the epidermal (early and late) progenitor populations (Supplemental

270 Figure 4C) (Wurtzel et al., 2015). Therefore, we next examined the epidermal and muscle cell

271   populations for defects in *yki(RNAi)* animals due to multiple dysregulated wound-induced genes

272   were expressed in these tissue types (Supplemental Figure 4C-D).

273

274   *yki(RNAi) animals show higher epidermal density and smaller cell size*

275   The epidermis is enriched for wound-induced genes and has a well-defined lineage that

276   can be readily assayed (Eisenhoffer et al., 2008b; Tu et al., 2015; van Wolfswinkel et al., 2014;

277   Wenemoser et al., 2012; Wurtzel et al., 2015; Zhu et al., 2015). Early epidermal progenitors

278   marked by *prog-2* were significantly increased in density in *yki(RNAi)* at 2 dpa. Similarly at 7

279   dpa, *yki(RNAi)* showed more $AGAT\text{-}1^+$ late epidermal progenitors and differentiated dorsal

280   epidermal cells compared to *control(RNAi)* (Figure 3A-B). This suggested that epidermal

281   differentiation is not blocked in *yki(RNAi)*, and instead, *yki* was required to restrict epidermal

282   numbers. The increased epidermal density in *yki(RNAi)* came at the expense of the cell size

283   (Figure 3C) and accordingly, the cell cortices of the epidermis were also smaller by

284   Concanavalin A staining (Figure 3D) (Zayas et al., 2010). This suggested that the increased

285   epidermal density may contribute to elevated wound-induced gene expression.

286

287   *An expanded population of muscle cells and patterning molecules are observed in yki(RNAi)*

288   *animals*

289   We next focused on the muscle population because it was the tissue with the most

290   dysregulated wound-induced genes in *yki(RNAi)*. Moreover, the $collagen^+$ muscle subpopulation

291   is the source of many patterning signals that predominantly belong to major signalling cascades

292   such as WNT, BMP, and TGF-β (Scimone et al., 2016; Witchley et al., 2013). In order to

293   understand the dynamics of the muscle cell population during regeneration, we administered

294   BrdU at 3fd15, amputated worms 5 days afterwards, and subsequently fixed them at 7 dpa

295   (Figure 4A). In *yki(RNAi)* animals, an increased number of *collagen*[+]/BrdU^{+} cells was observed

296   compared to controls (Figure 4B-C). Accordingly, we found that *collagen* and *troponin*, another

297   muscle-specific gene, were upregulated immediately after injury in *yki(RNAi)* tail fragments by

298   qRT-PCR (Figure 4D). Thus, the increased muscle cell population could also account for the

299   augmented and aberrant transcriptional wound response in *yki(RNAi)*.

300   To test whether the overproduction of muscle cells in *yki(RNAi)* was attributed to

301   increased wound-induced gene expression, we examined *wnt1*. Injury induces *wnt1* expression,

302   but it is also a polarity determinant that has >90% co-localization within the *collagen*+ muscle

303   cell population (Petersen and Reddien, 2009; Witchley et al., 2013). In *yki(RNAi)* animals at 6

304   and 12 hpa, significantly more *wnt1*^{+} cells were observed along the tail midline, but also

305   ectopically at the wound margin (Figure 4E). These ectopic *wnt1*^{+} cells were predominantly

306   *collagen*[+] with no significant difference in the percentage of *wnt1*[+]/*collagen*^{-} cells in *yki(RNAi)* as

307   compared to *control(RNAi)* (14.2±3.9% and 11.8±8.1%, respectively; *p*=0.39) (Figure 4F-G).

308   Therefore, the increased *wnt1*^{+} cells in *yki(RNAi)* tails were not ectopically expressed in a

309   different cell type and suggested that the expanded muscle population can be attributed to the

310   expanded expression of wound-induced genes.

311   Many non-wound-induced body patterning molecules are also known to be highly

312   expressed in *collagen*^{+} cells, including the HOXs and FGFs (Scimone et al., 2016; Witchley et

313   al., 2013). With the increased muscle population in *yki(RNAi)* animals, we tested whether other

314   wound and non-wound induced patterning molecules were aberrantly expressed. By pair-wise

315   DEseq2 analyses between *yki(RNAi)* and *control(RNAi)* matched time points, we found 35

316   patterning genes significantly changing at any given time point ([FC] > 1.2 or [FC] < 0.83 with

14

317   [FDR] < 0.05) (Figure 4H and Supplemental Table 3). A high proportion of these genes were

318   associated with WNT signalling—a key determinant in anterior-posterior identity—which was

319   expected because *yki(RNAi)* tails do not regenerate their anterior (Lin and Pearson, 2014).

320   However, *notum*, which antagonizes WNT signalling to promote head specification, as well as

321   the anteriorly-expressed *sfrp-2* were still expressed in *yki(RNAi)* tails (Figure 4H and

322   Supplemental Figure 5A-B). Thus, the *yki(RNAi)* regenerative defects were not simply a failure

323   to express anterior-specification genes. Indeed, the changes in patterning were not limited to the

324   WNTs, but also included molecules associated with patterning the midline such as *slit-1* and

325   *netrin-2A* (Supplemental Figure 5C), or the dorsal-ventral axis such as *bmp*, *tolloid-1*, *noggin-1*,

326   and *-7* (Figure 4H). Alterations in expression of signalling pathways can affect tissue

327   maintenance with improperly sized organs, thus, we next tested whether *yki(RNAi)* animals had

328   defects in organ scaling (Hill and Petersen, 2015; Reddien, 2011; Scimone et al., 2016).

329

330   *yki(RNAi) animals exhibit defects in scaling and morphallaxis*

331   The planarian has an innate ability to sense injury size by recognizing the amount of

332   tissue removed, known as the "missing tissue response" or "size sensing mechanism" (Gaviño et

333   al., 2013). We wanted to test whether this mechanism was still in place in *yk(RNAi)* animals

334   because the injury responses were heightened, prolonged, and sustained (Figures 1 and 2). The

335   regenerating planarian pharynx is an ideal organ to test for the animal's ability to sense the size

336   of wounds. In relation to the amount of tissue removed or amputated, the post-mitotic planarian

337   pharynx must be rescaled and re-patterned to its new fragment size, which is accomplished in

338   part by changes in cell death (Pellettieri et al., 2010). To test how this scaling mechanism may be

339   altered in *yki(RNAi)*, pharynxes were chemically amputated from worms that had been

15

340   regenerating for 3 days but underwent selective amounts of tissue removal (0%, 10%, 40%, and

341   80%) (Figure 5A). The isolated pharynxes were immediately fixed and assayed for TUNEL

342   (Figure 5B). In *control(RNAi)* amputated pharynxes, a proportionality between the amount of

343   tissue removed and the amount of cell death was observed, as previously reported (Figure 5B).

344   However, in *yki(RNAi)*, this relationship was uncoupled (Figure 5B-C). This suggested that *yki*

345   was required to mediate a scaling process or injury-size sensing mechanism during the initial

346   stages of regeneration.

347   The role for *yki* to mediate scaling can also be assayed during the process of morphallaxis

348   or re-scaling of body and tissue proportions. For example, similar to the pharynx in trunk

349   fragments, the planarian brain must be scaled down in size in relation to the new size of the head

350   fragment (Hill and Petersen, 2015; Morgan, 1898; Reddien and Alvarado, 2004). Using DAPI

351   and *chat* (*choline acetyltransferase)*, which specifically labels mature cholinergic neurons, a

352   ratio of the brain size relative to the body size was determined (Figure 5D) (Agata et al., 1998).

353   At 14 dpa, *yki(RNAi)* head fragments were smaller due to a regeneration defect (Lin and Pearson,

354   2014), however, its brain to body size was significantly larger (Figure 5E). Accordingly, *cintillo*,

355   which is expressed in chemoreceptive neurons, also did not maintain scale in *yki(RNAi)* animals

356   (Figure 5F) (Hill and Petersen, 2015; Sanchez Alvarado et al., 2002). Similarly, the *slit* midline

357   gradient was also enlarged in *yki(RNAi)* at 14 dpa in all three regenerating fragments (Figure 5G)

358   (Cebria et al., 2007). Finally, *yki(RNAi)* animals with an eye injury showed a heightened

359   transcriptional injury response and regenerated significantly larger compared to the contralateral

360   uninjured one (Supplemental Figure 6). Taken together, this suggested that *yki* was required to

361   determine organ scaling by restricting the magnitude and duration of injury responses (Figure 6).

362

Discussion

363

364   Regeneration is a complex, multistep process that requires precise spatial and temporal

365 regulation. The first step is an injury response comprised of a burst of proliferation, apoptosis,

366 and a transcriptional injury response, which together provide the initial basis for planarian

367 regeneration (Pellettieri et al., 2010; Wenemoser et al., 2012; Wenemoser and Reddien, 2010;

368 Wurtzel et al., 2015). The transcriptional injury response is a generic and robust program that is

369 activated immediately following any type of injury, whereby failures of activation have

370 ramifications during regeneration (Almuedo-Castillo et al., 2014; Wenemoser et al., 2012;

371 Wurtzel et al., 2015). Here, we demonstrate that *yki* is required to restrict this response (Figure

372 6). In all three *yki(RNAi)* regenerating fragments, wound-induced genes were precociously

373 expressed earlier with a heighted response evident by WISH, qRT-PCR, and RNAseq (Figure

374 2A-K). This aberrant signalling of mitogens, transcription factors, and patterning molecules may

375 subsequently affect the proliferative kinetics. Although the signal(s) that induce the bimodal

376 waves of proliferation remain elusive in planarians, correlations between the transcriptional and

377 proliferative response may be inferred. First, the two responses overlap temporally (Wenemoser

378 et al., 2012; Wenemoser and Reddien, 2010; Wurtzel et al., 2015). Second, *follistatin(RNAi)*

379 regenerating animals fail to express a second wave of wound-induced genes and also fail to

380 mount a second burst of proliferation, suggesting a possible link between the two processes

381 (Gaviño et al., 2013; Roberts-Galbraith and Newmark, 2013). In addition, previous work

382 profiling liver regeneration identified waves of transcription that prime hepatocytes for

383 subsequent proliferation (Fausto, 2000; Haber et al., 1993; Su et al., 2002). Therefore, a similar

384 mechanism may be occurring in planarians, whereby the transcriptional injury response is

385 required to initiate proper regenerative proliferative kinetics.

386   Along with an altered transcriptional injury response, *yki(RNAi)* animals also showed

387   dysregulated proliferation patterns. Normally, proliferation occurs in a bimodal wave

388   (Wenemoser and Reddien, 2010), however in *yki(RNAi)*, the first peak was significantly

389   increased and prolonged, while the second one was delayed and similarly heighted (Figure 1A-

390   B). These altered temporal patterns are reminiscent to the changes also observed in the

391   transcriptional injury response, suggesting a possible relationship between the two. Moreover,

392   the changes in proliferation may not be cell autonomous because *yki* is not enriched the stem

393   cells (Figure 1G) (Lin and Pearson, 2014; Wurtzel et al., 2015). The stem cell subclass identities

394   of the proliferating population remained unchanged in *yki(RNAi)*, suggesting that *yki* does not

395   affect stem cell lineage commitment. Indeed, differentiation proceeded at even higher levels in

396   *yki(RNAi)* (Figure 3, epidermal; Figure 4, muscle). Therefore, the global increase in proliferating

397   stem cells may be attributed to a cell non-autonomous factor, perhaps from the increased

398   transcriptional injury response. Congruent with this hypothesis, proliferation was sustained at the

399   wound margin at 72 hpa in *yki(RNAi)*, whereas it normally occurs more posteriorly in

400   *control(RNAi)* at this time point (Figure 1E). Perhaps this role of *yki* in planarians is similar to

401   *Drosophila* midgut regeneration where Yki is activated in the non-proliferative enterocytes to

402   secrete cytokines that stimulate intestinal stem cell proliferation in a non-autonomous fashion

403   (Karpowicz et al., 2010; Shaw et al., 2010; Staley and Irvine, 2010). Similarly, axolotl limb

404   regenerative proliferation is regulated by non-autonomous cues, such as the secreted molecule

405   MARCKS that is also transcriptionally injury-induced, although it is unknown whether a *yorkie*

406   homolog is involved (Sugiura et al., 2016). Future studies elucidating what the injury-induced

407   molecule that triggers proliferation would provide great insights into initiation of regenerative

408   programs in planarians.

409   Another key feature of the transcriptional injury response is to lay the foundation for

410   axial and tissue re-scaling. The 12 hpa time point is the peak temporal expression window for the

411   majority of wound-induced patterning molecules (Wenemoser et al., 2012; Wurtzel et al., 2015),

412   including *wnt1* which is crucial in determining axial polarity (Petersen and Reddien, 2009).

413   Interestingly, many of the dysregulated wound-induced genes in *yki(RNAi)* have roles in

414   patterning (Figure 2H-I). Indeed, *wnt1* was significantly increased in *yki(RNAi)* animals (Figure

415   3G). Modulating patterning can have consequences in regeneration by affecting pole

416   determination, cell fate decisions, or organ sizing and scaling (Currie et al., 2016b; Gurley et al.,

417   2008; Hill and Petersen, 2015; Lander and Petersen, 2016; Scimone et al., 2016; Scimone et al.,

418   2014). We hypothesize that the failures in regeneration in *yki(RNAi)* may be attributed to the

419   mis-expression of multiple patterning molecules (Figure 4H). In addition, the process of

420   morphallaxis was also altered in *yki(RNAi)* (Figure 5D-G). Therefore, the dysregulated

421   transcriptional injury response in *yki(RNAi)* may be responsible for the changes in proliferation

422   and patterning that likely have detrimental effects on scaling and sizing during regeneration

423   (Figure 6).

424   What could be causing the upregulation of the transcriptional injury response in

425   *yki(RNAi)* animals? One possibility may be epithelial integrity which serves as a negative

426   feedback regulator of the transcriptional injury responses. *Smed-egr-5(RNAi)* (*early growth*

427   *factor 5*), a crucial post-mitotic epidermal determinant, causes a loss of epithelial integrity and

428   increased wound-induced gene expression (Tu et al., 2015). Similarly, *yki(RNAi)* animals had

429   increased epidermal density concurrent with increased wound-induced gene expression (Figure

430   3A-D). In other systems, the roles for YAP in regulating cell density converge upon inputs such

431   as cytoskeletal tension and mechanosensation (Dupont et al., 2011; Halder et al., 2012); yet, how

432 tension may function in planarian biology, or in a regenerative context, remains unknown. In

433 addition, other upstream cues may be other previously characterized pathways that have roles in

434 regulating the planarian injury responses, including TGFβ signalling through the Activin-

435 Follistatin axis, SMG-1 and mTORC, and JNK signalling (Almuedo-Castillo et al., 2014; Gaviño

436 et al., 2013; González-Estévez et al., 2012). Yki/YAP also have described roles in interacting

437 with each of these pathways, however, the interactions remain to be biochemically elucidated in

438 planarians (Attisano and Wrana, 2013; Codelia et al., 2014; Csibi and Blenis, 2012; Sun and

439 Irvine, 2013). Therefore, multiple wounding cues may converge on Yki to direct the injury

440 responses. Taken together, we have shown that Yki is required to restrict the magnitude and

441 duration of the injury responses, which coordinate proliferation to replace the missing tissue and

442 patterning to integrate the newly differentiated cells; thus, Yki is essential in injury signalling

443 that ultimately dictates scaling.

444
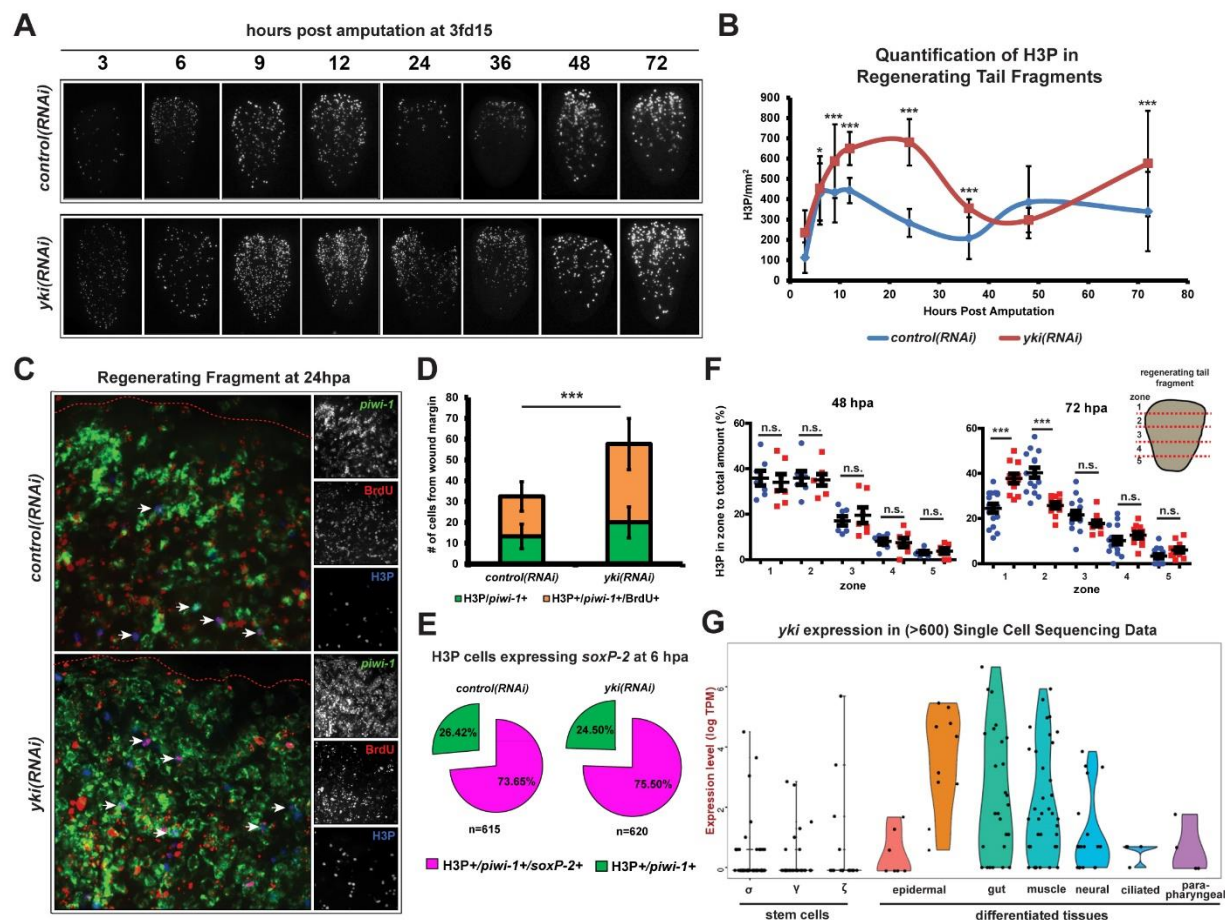
Figure 1. *yki* **regulates stem cell proliferation dynamics during regeneration.** (A) Time course of regenerating fragments stained with mitotic marker, phosphorylated histone 3 (H3P). (B) The quantification of time course in A. (C) *yki(RNAi)* does not affect the cell cycle. Triple positive cells (H3P+/*piwi-1*+/BrdU+) are marked with white arrows. Red dotted line is the wound boundary. (D) No significant difference is observed (*p*=0.67) in the percentage of H3P+/*piwi-1*+/BrdU+ cells (orange bar) to the total amount of H3P cells (orange and green bars summed) in *control(RNAi)* compared to *yki(RNAi)* tail fragments (59±9% and 60±7%, respectively). (E) Percentages of H3P+/*piwi-1*+ cells expression sigma stem cell marker *soxP-2* (pink) or not (green). (F) The percentage of mitoses occurring in each zone compared to the total amount at 48 and 72 hpa in *control(RNAi)* (blue) and *yki(RNAi)* (red). Zones are divided into 5 equal compartments (20% each) with zone 1 at the anterior, closest to the wound site. (G) From single-cell RNAseq, *yki* expression is enriched in the differentiated tissues (epidermal, gut, and muscle), and is lowly expressed in the stem cell compartment. Data show mean ± s.d. n.s.=not significat, *$p<0.05$, **<$p<0.01$, ***$p<0.001$.
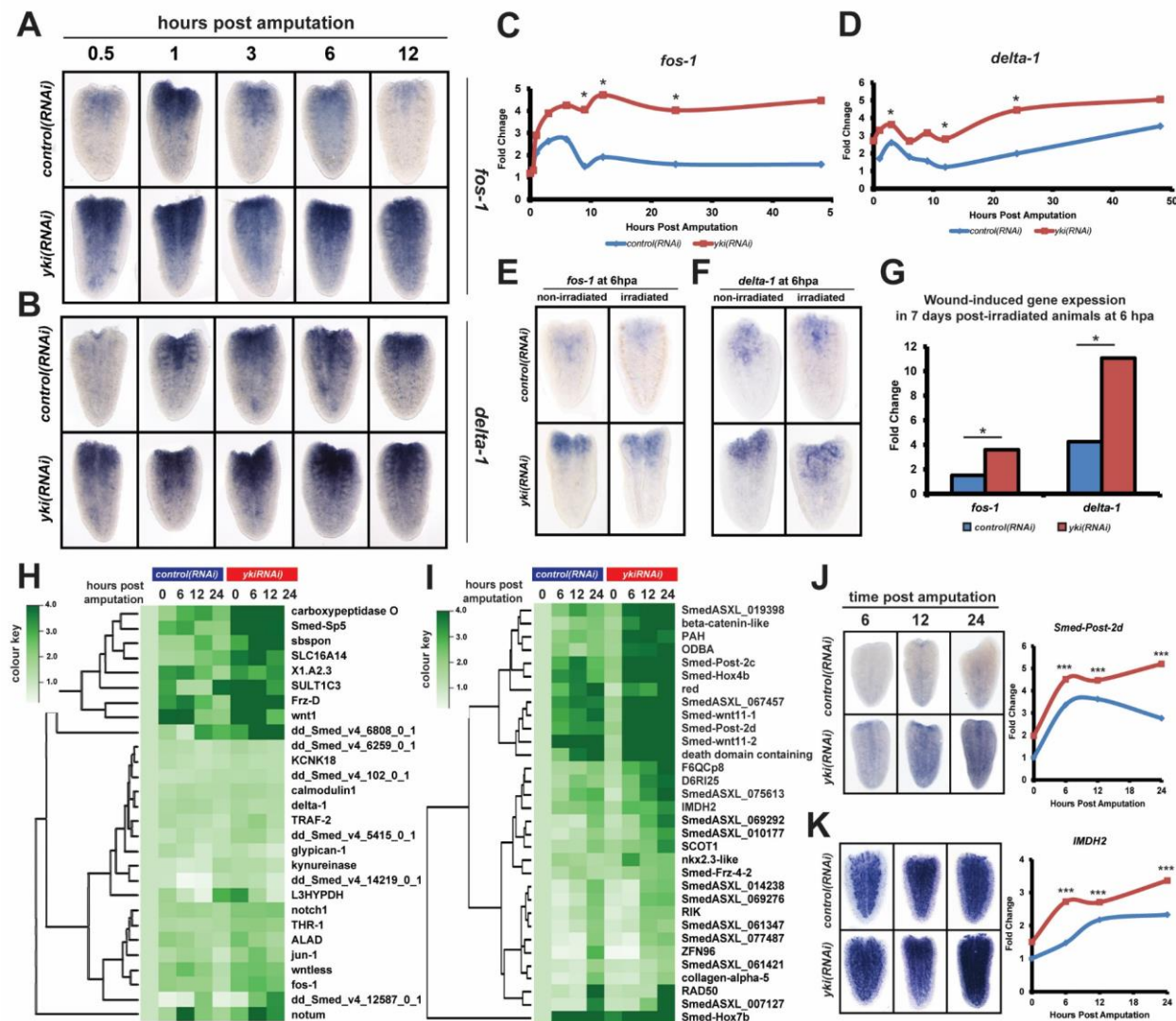
Figure 2. *yki* is required to restrict the transcriptional injury response. (A-B) A WISH time course of wound-induced genes *fos-1* (A) and *delta-1* (B) during regeneration. (C-D) qRT-PCR experiments parallel results by WISH in A. (E-G) Irradiated worms show the same *fos-1* (E) and *delta-1* (F) response as non-irradiated worms by WISH (E-F) and qRT-PCR (G). (H) A heatmap of significantly upregulated (fold change [FC] > 1.2, false discovery rate [FDR] < 0.05, pair-wise comparison between matched time points) *bona fide* wound-induced genes normalized to *control(RNAi)* intact levels (I) Heatmap of novel wound-induced genes with [FC] normalized to *control(RNAi)* intacts. (J-K) Regeneration time course stained by WISH (left) with corresponding CPM fold-change normalized to *control(RNAi)* intact (right) for: *Smed-Post-2d* (J) and *IMDH2* (K). *$p<0.05$, **$p<0.01$.

22
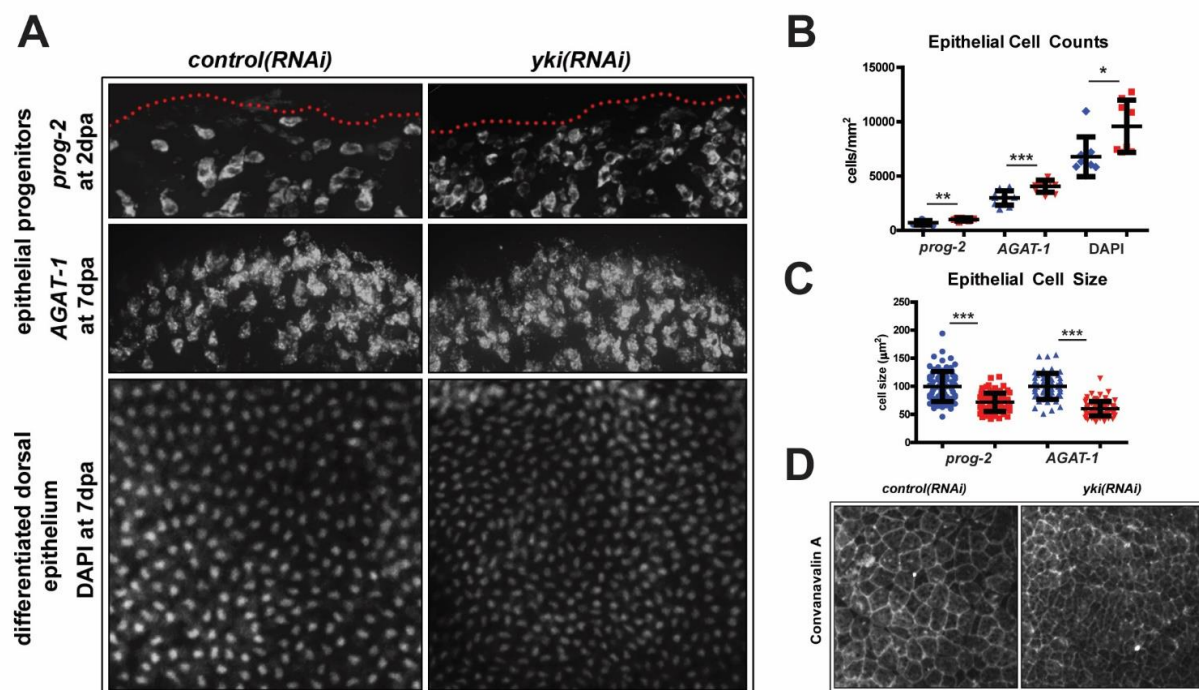
Figure 3. *yki* restricts epidermal density and cell size. (A-C) Epidermal populations assayed with *prog-2* at 2 dpa, and *AGAT-1* and DAPI at 7 dpa by WISH (A). Red dotted line indicates wound margin. Histogram of epidermal cell counts (B) and cell sizes (C) by quantifying images in A. Blue symbols are *control(RNAi)* and red is for *yki(RNAi)*. (D) Epidermal junctions stained with Concanavalin A. Data show mean ± s.d. *$p<0.05$, **$p<0.01$, ***$p<0.001$.
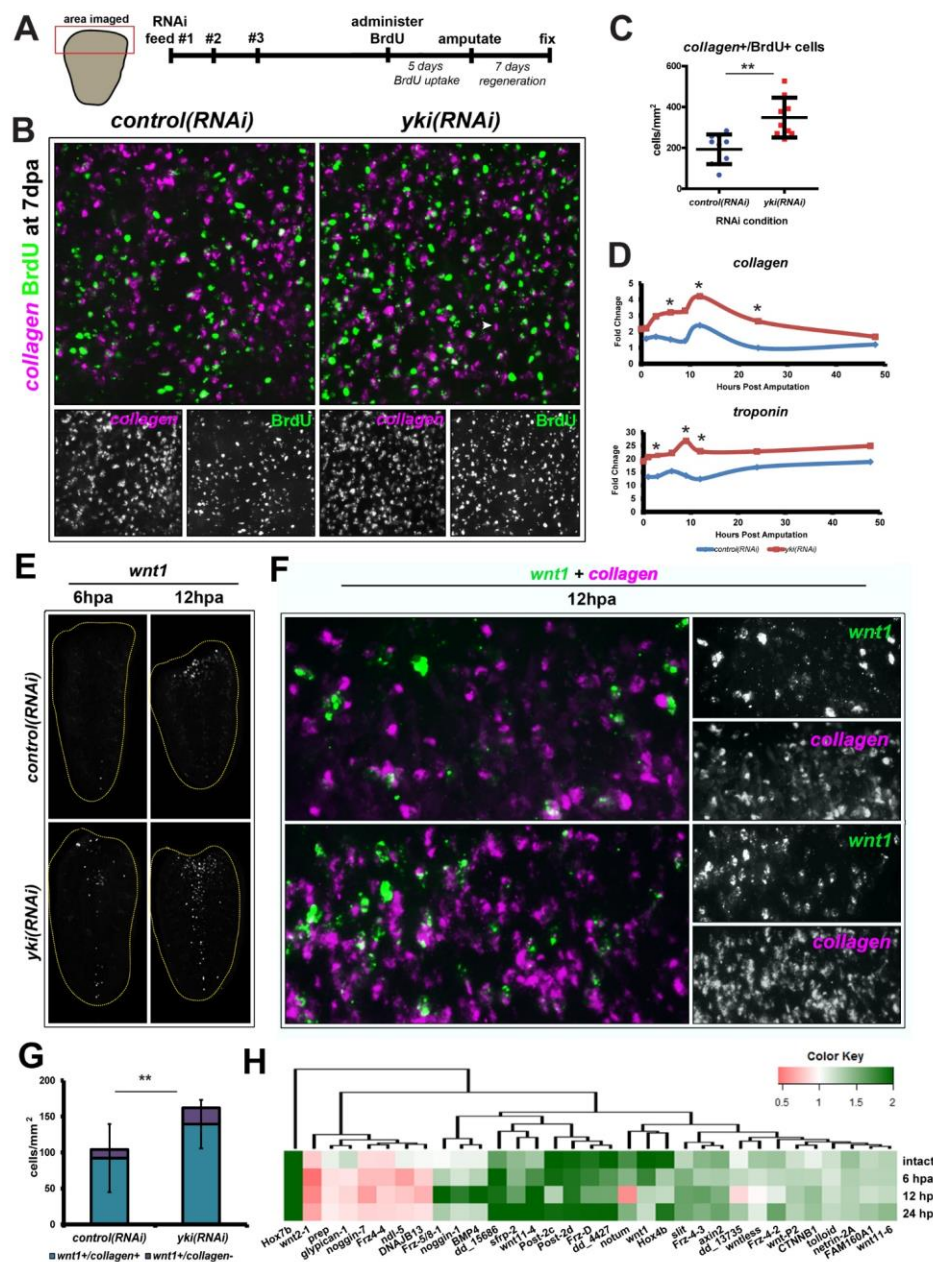
481

Figure 4. *yki(RNAi)* **causes an expansion of the muscle population and mis-expression of patterning molecules, including** *wnt-1*. (A-C) BrdU chases into the *collagen*+ muscle population. A timeline of the BrdU experiment (A). FISH for *collagen* (magenta) and BrdU (green) (B) with double positive cells quantified in a histogram (C). (D) qRT-PCR for *collagen* and *troponin* during a regeneration time course. (E) *wnt1* expression at 6 hpa and 12 hpa by WISH. Yellow dotted line outlines the worm fragment. (F) dFISH of *wnt1* (green) and *collagen* (magenta). (G) A quantification of *wnt1*+ cells that are *collagen*+ (turquoise) and *collagen*- (purple) at 12 hpa. A significant difference in the total number (turquoise + purple bars summed) is observed in *yki(RNAi)*. (H) The fold change of significantly changing patterning genes in *yki(RNAi)* compared to *control(RNAi)* in intacts, 6, 12, and 24 hpa (FDR < 0.05). Data show mean ± s.d. *$p<0.05$, **$p<0.01$.
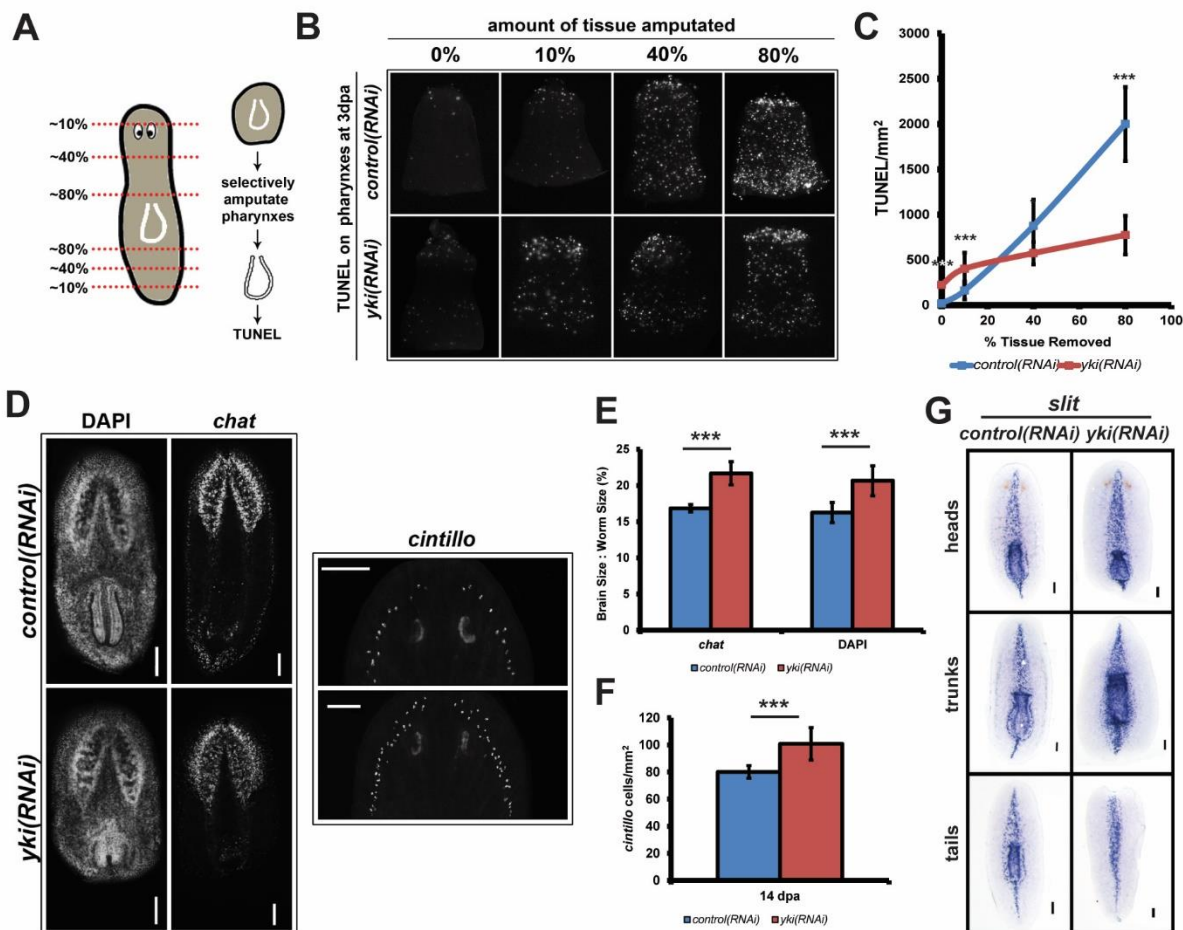
24

493

Figure 5. *yki* regulates scaling and morphallaxis. (A) Pharynxes amputated from animals with selective tissue removed can be assayed for cell death as a size sensing mechanism. A schematic of the regeneration series with various percentages of tissue removed with subsequent experimental steps outlined. (B) Amputated pharynxes assayed for TUNEL. (C) Quantification of TUNEL stained pharynxes from A. (D) Head fragments from *control(RNAi)* and *yki(RNAi)* worms were assayed for brain size and morphology with DAPI, *chat*, and *cintillo* at 14 dpa. Scale bar is 100 μm. (E) The ratio of brain size to worm size expressed as a percentage and quantified from D. (F) Quantification of the number of *cintillo*+ cells to worm size from E. (G) Regenerating fragments at 14 dpa stained with *slit*. *yki(RNAi)* animals show an expanded *slit* gradient that fails to rescale to appropriate proportions. Data show mean ± s.d. *$p<0.05$, ***$p<0.001$.
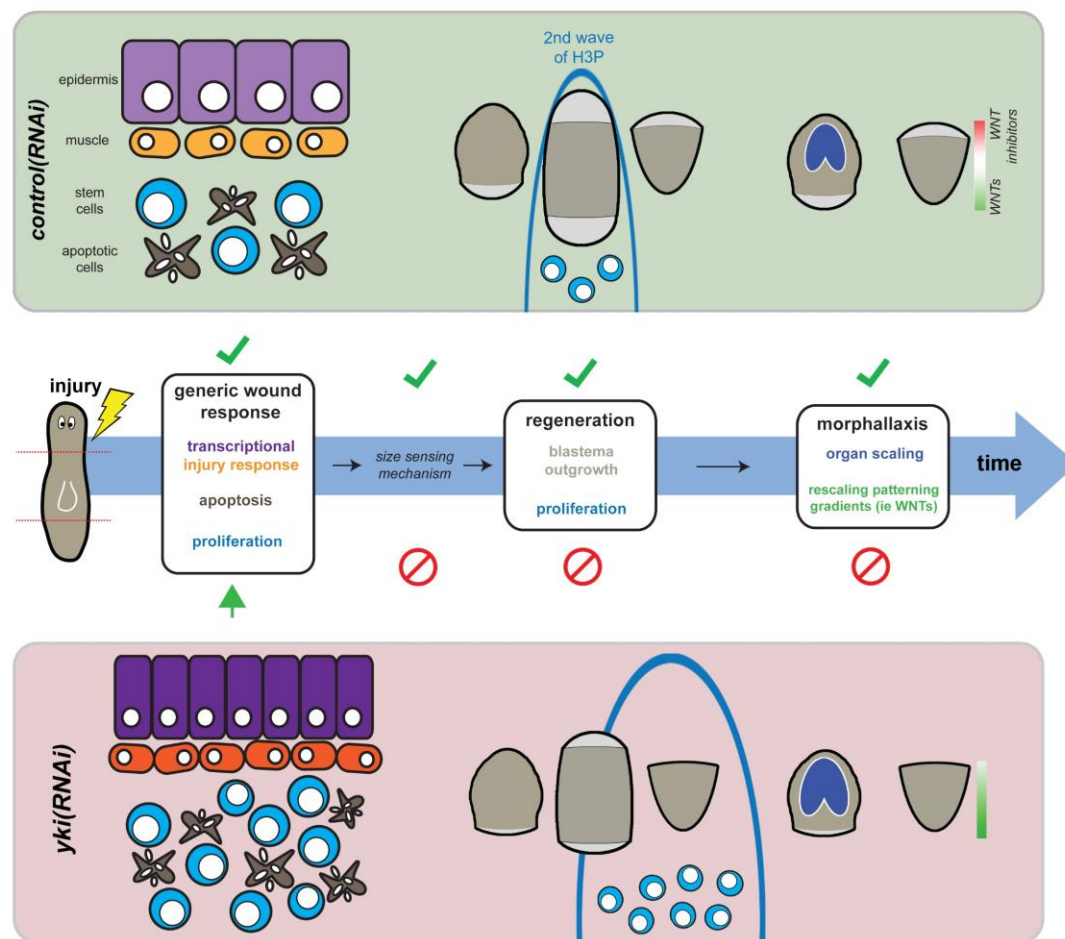
505

25

506

Figure 6. The roles for *yki* during planarian regeneration. Top, green: When the planarian is injured, it undergoes a generic wound response composed of: a transcriptional injury response that primarily localizes to the epidermis and muscle, and a burst of proliferation and apoptosis. A subsequent "missing tissue response" or "a size-sensing mechanism" recognizes the amount of tissue loss to initiate regenerative programs. This entails a second burst of proliferation and blastema outgrowth. After the lost tissues have been replaced, reintegration with the old tissues occurs by morphallaxis. For example, the brain will be rescaled down in size in head fragments, and the WNT genes re-establish their graded expression along the anterior-posterior axis. Bottom, red: By contrast in *yki(RNAi)* regenerating animals, all aspects of the generic wound response are heightened, evident by dysregulation proliferative and apoptotic dynamics, and augmented wound-induced gene expression, likely attributed to the increased epithelial and muscle cell numbers. The "missing tissue response" or the "size sensing mechanism" is also uncoupled in *yki(RNAi)*, suggesting that size and scaling may be altered. Moreover, the second mitotic burst is temporally shifted and a failure in regeneration is observed. Ultimately, repatterning and scaling are also affected. Altogether, *yki* is required to restrict multiple aspects the injury response, including proliferation, wound-induced gene expression, and patterning to ensure proper regenerative outcomes.

524

26

References

Adler, C. E., Seidel, C. W., McKinney, S. A. and Alvarado, A. (2014). Selective amputation of the pharynx identifies a FoxA-dependent regeneration program in planaria. *Elife* **3**.

Agata, K., Soejima, Y., Kato, K., Kobayashi, C., Umesono, Y. and Watanabe, K. (1998). Structure of the planarian central nervous system (CNS) revealed by neuronal cell markers. *Zoolog Sci* **15**, 433-40.

Almuedo-Castillo, M., Crespo, X., Seebeck, F., Bartscherer, K., Salò, E. and Adell, T. (2014). JNK Controls the Onset of Mitosis in Planarian Stem Cells and Triggers Apoptotic Cell Death Required for Regeneration and Remodeling. *PLoS genetics* **10**.

Attisano, L. and Wrana, J. L. (2013). Signal integration in TGF-beta, WNT, and Hippo pathways. *F1000Prime Rep* **5**, 17.

Barry, E. R., Morikawa, T., Butler, B. L., Shrestha, K., de la Rosa, R., Yan, K. S., Fuchs, C. S., Magness, S. T., Smits, R., Ogino, S. et al. (2012). Restriction of intestinal stem cell expansion and the regenerative response by YAP. *Nature*.

Camargo, F. D., Gokhale, S., Johnnidis, J. B., Fu, D., Bell, G. W., Jaenisch, R. and Brummelkamp, T. R. (2007). YAP1 increases organ size and expands undifferentiated progenitor cells. *Current biology : CB* **17**, 2054-2060.

Cebria, F., Guo, T., Jopek, J. and Newmark, P. A. (2007). Regeneration and maintenance of the planarian midline is regulated by a slit orthologue. *Dev Biol* **307**, 394-406.

Codelia, V. A., Sun, G. and Irvine, K. D. (2014). Regulation of YAP by mechanical strain through Jnk and Hippo signaling. *Curr Biol* **24**, 2012-7.

Cowles, M. W., Brown, D. D., Nisperos, S. V., Stanley, B. N., Pearson, B. J. and Zayas, R. M. (2013). Genome-wide analysis of the bHLH gene family in planarians identifies factors required for adult neurogenesis and neuronal regeneration. *Development (Cambridge, England)* **140**, 4691-4702.

Csibi, A. and Blenis, J. (2012). Hippo-YAP and mTOR pathways collaborate to regulate organ size. *Nat Cell Biol* **14**, 1244-5.

Currie, K. W., Brown, D. D., Zhu, S., Xu, C., Voisin, V., Bader, G. D. and Pearson, B. J. (2016a). HOX gene complement and expression in the planarian Schmidtea mediterranea. *Evodevo* **7**, 7.

Currie, K. W., Molinaro, A. M. and Pearson, B. J. (2016b). Neuronal sources of hedgehog modulate neurogenesis in the adult planarian brain. *Elife* **5**.

Dong, J., Feldmann, G., Huang, J., Wu, S., Zhang, N., Comerford, S. A., Gayyed, M. F., Anders, R. A., Maitra, A. and Pan, D. (2007). Elucidation of a universal size-control mechanism in Drosophila and mammals. *Cell* **130**, 1120-1133.

Dupont, S., Morsut, L., Aragona, M., Enzo, E., Giulitti, S., Cordenonsi, M., Zanconato, F., Digabel, J., Forcato, M., Bicciato, S. et al. (2011). Role of YAP/TAZ in mechanotransduction. *Nature* **474**, 179-183.

Eisenhoffer, G., Kang, H. and Sánchez Alvarado, A. (2008a). Molecular analysis of stem cells and their descendants during cell turnover and regeneration in the planarian Schmidtea mediterranea. *Cell stem cell* **3**, 327-339.

Eisenhoffer, G. T., Kang, H. and Alvarado, A. (2008b). Molecular analysis of stem cells and their descendants during cell turnover and regeneration in the planarian Schmidtea mediterranea. *Cell stem cell* **3**, 327-339.

Elliott, S. A. and Alvarado, A. (2013). The history and enduring contributions of planarians to the study of animal regeneration. *Wiley interdisciplinary reviews. Developmental biology* **2**, 301-326.

Gaviño, M. A., Wenemoser, D., Wang, I. E. and Reddien, P. W. (2013). Tissue absence initiates regeneration through Follistatin-mediated inhibition of Activin signaling. *Elife* **2**.

González-Estévez, C., Felix, D. A., Smith, M. D., Paps, J., Morley, S. J., James, V., Sharp, T. V. and Aboobaker, A. A. (2012). SMG-1 and mTORC1 Act Antagonistically to Regulate Response to Injury and Growth in Planarians. *PLoS genetics* **8**.

Gurley, K. A., Elliott, S. A., Simakov, O., Schmidt, H. A., Holstein, T. W. and Alvarado, A. (2010). Expression of secreted Wnt pathway components reveals unexpected complexity of the planarian amputation response. *Developmental biology* **347**, 24-39.

Gurley, K. A., Rink, J. C. and Alvarado, A. (2008). Beta-catenin defines head versus tail identity during planarian regeneration and homeostasis. *Science (New York, N.Y.)* **319**, 323-327.

Halder, G., Dupont, S. and Piccolo, S. (2012). Transduction of mechanical and cytoskeletal cues by YAP and TAZ. *Nature reviews. Molecular cell biology* **13**, 591-600.

Halder, G. and Johnson, R. L. (2011). Hippo signaling: growth control and beyond. *Development (Cambridge, England)* **138**, 9-22.

Hill, E. M. and Petersen, C. P. (2015). Wnt/Notum spatial feedback inhibition controls neoblast differentiation to regulate reversible growth of the planarian brain. *Development* **142**, 4217-29.

Holstein, T. W., Hobmayer, E. and Technau, U. (2003). Cnidarians: an evolutionarily conserved model system for regeneration? *Dev Dyn* **226**, 257-67.

Huang, J., Wu, S., Barrera, J., Matthews, K. and Pan, D. (2005). The Hippo signaling pathway coordinately regulates cell proliferation and apoptosis by inactivating Yorkie, the Drosophila Homolog of YAP. *Cell* **122**, 421-434.

Iglesias, M., Gomez-Skarmeta, J. L., Salo, E. and Adell, T. (2008). Silencing of Smed-betacatenin1 generates radial-like hypercephalized planarians. *Development* **135**, 1215-21.

Karpowicz, P., Perez, J. and Perrimon, N. (2010). The Hippo tumor suppressor pathway regulates intestinal stem cell regeneration. *Development* **137**, 4135-45.

Lander, R. and Petersen, C. P. (2016). Wnt, Ptk7, and FGFRL expression gradients control trunk positional identity in planarian regeneration. *Elife* **5**.

Langmead, B. and Salzberg, S. L. (2012). Fast gapped-read alignment with Bowtie 2. *Nat Methods* **9**, 357-9.

Lauter, G., Soll, I. and Hauptmann, G. (2011). Two-color fluorescent in situ hybridization in the embryonic zebrafish brain using differential detection systems. *BMC Dev Biol* **11**, 43.

Lin, A. Y. and Pearson, B. J. (2014). Planarian yorkie/YAP functions to integrate adult stem cell proliferation, organ homeostasis and maintenance of axial patterning. *Development (Cambridge, England)* **141**, 1197-1208.

Love, M. I., Huber, W. and Anders, S. (2014). Moderated estimation of fold change and dispersion for RNA-seq data with DESeq2. *Genome Biol* **15**, 550.

Macosko, E. Z., Basu, A., Satija, R., Nemesh, J., Shekhar, K., Goldman, M., Tirosh, I., Bialas, A. R., Kamitaki, N., Martersteck, E. M. et al. (2015). Highly Parallel Genome-wide Expression Profiling of Individual Cells Using Nanoliter Droplets. *Cell* **161**, 1202-14.

Molinaro, A. M. and Pearson, B. J. (2016). In silico lineage tracing through single cell transcriptomics identifies a neural stem cell population in planarians. *Genome Biology* **17**, 1-17.

Morgan, T. (1898). Experimental studies of the regeneration of Planaria maculata. *Development Genes and Evolution* **7**, 364-397.

Morgan, T. H. (1901). Growth and regeneration in Planaria lugubris. *Archiv für Entwickelungsmechanik der Organismen* **13**.

Newmark, P., Reddien, P., Cebrià, F. and Sánchez Alvarado, A. (2003). Ingestion of bacterially expressed double-stranded RNA inhibits gene expression in planarians. *Proceedings of the National Academy of Sciences of the United States of America* **100 Suppl 1**, 11861-11865.

Pearson, B. and Sánchez Alvarado, A. (2010). A planarian p53 homolog regulates proliferation and self-renewal in adult stem cell lineages. *Development (Cambridge, England)* **137**, 213-221.

Pearson, B. J., Eisenhoffer, G. T., Gurley, K. A., Rink, J. C., Miller, D. E. and Sanchez Alvarado, A. (2009). Formaldehyde-based whole-mount in situ hybridization method for planarians. *Dev Dyn* **238**, 443-50.

619 **Pellettieri, J., Fitzgerald, P., Watanabe, S., Mancuso, J., Green, D. R. and Alvarado, A.** (2010). Cell death
620 and tissue remodeling in planarian regeneration. *Developmental biology* **338**, 76-85.
621 **Petersen, C. P. and Reddien, P. W.** (2009). A wound-induced Wnt expression program controls planarian
622 regeneration polarity. *Proceedings of the National Academy of Sciences of the United States of America*
623 **106**, 17061-17066.
624 **Reddien, P. W.** (2011). Constitutive gene expression and the specification of tissue identity in adult
625 planarian biology. *Trends in genetics : TIG* **27**, 277-285.
626 **Reddien, P. W. and Alvarado, A.** (2004). Fundamentals of planarian regeneration. *Annual review of cell*
627 *and developmental biology* **20**, 725-757.
628 **Reuter, H., März, M., Vogg, M. C., Eccles, D., Grífol-Boldú, L., Wehner, D., Owlarn, S., Adell, T.,**
629 **Weidinger, G. and Bartscherer, K.** (2014). β-Catenin-Dependent Control of Positional Information along
630 the AP Body Axis in Planarians Involves a Teashirt Family Member. *Cell reports*.
631 **Rinkevich, Y., Lindau, P., Ueno, H., Longaker, M. T. and Weissman, I. L.** (2011). Germ-layer and lineage-
632 restricted stem/progenitors regenerate the mouse digit tip. *Nature* **476**, 409-13.
633 **Roberts-Galbraith, R. H. and Newmark, P. A.** (2013). Follistatin antagonizes activin signaling and acts
634 with notum to direct planarian head regeneration. *Proc Natl Acad Sci U S A* **110**, 1363-8.
635 **Saló, E. and Baguna, J.** (1989). Regeneration and pattern formation in planarians. II. and role of cell
636 movements in blastema formation. *Development*.
637 **Sanchez Alvarado, A.** (2000). Regeneration in the metazoans: why does it happen? *Bioessays* **22**, 578-
638 90.
639 **Sánchez Alvarado, A.** (2002). The Schmidtea mediterranea database as a molecular resource for
640 studying platyhelminthes, stem cells and regeneration. *Development* **129**.
641 **Sanchez Alvarado, A., Newmark, P. A., Robb, S. M. and Juste, R.** (2002). The Schmidtea mediterranea
642 database as a molecular resource for studying platyhelminthes, stem cells and regeneration.
643 *Development* **129**, 5659-65.
644 **Scimone, M. L., Cote, L. E., Rogers, T. and Reddien, P. W.** (2016). Two FGFRL-Wnt circuits organize the
645 planarian anteroposterior axis. *Elife* **5**.
646 **Scimone, M. L., Lapan, S. W. and Reddien, P. W.** (2014). A forkhead transcription factor is wound-
647 induced at the planarian midline and required for anterior pole regeneration. *PLoS genetics* **10**.
648 **Shaw, R. L., Kohlmaier, A., Polesello, C., Veelken, C., Edgar, B. A. and Tapon, N.** (2010). The Hippo
649 pathway regulates intestinal stem cell proliferation during Drosophila adult midgut regeneration.
650 *Development* **137**, 4147-58.
651 **Staley, B. K. and Irvine, K. D.** (2010). Warts and Yorkie mediate intestinal regeneration by influencing
652 stem cell proliferation. *Curr Biol* **20**, 1580-7.
653 **Sugiura, T., Wang, H., Barsacchi, R., Simon, A. and Tanaka, E. M.** (2016). MARCKS-like protein is an
654 initiating molecule in axolotl appendage regeneration. *Nature* **531**, 237-240.
655 **Sun, G. and Irvine, K. D.** (2013). Ajuba family proteins link JNK to Hippo signaling. *Sci Signal* **6**, ra81.
656 **Takeo, M., Chou, W. C., Sun, Q., Lee, W., Rabbani, P., Loomis, C., Taketo, M. M. and Ito, M.** (2013).
657 Wnt activation in nail epithelium couples nail growth to digit regeneration. *Nature* **499**, 228-32.
658 **Thornton, C. S.** (1968). Amphibian limb regeneration. *Adv Morphog* **7**, 205-49.
659 **Tu, K. C., Cheng, L. C., Vu, H. T. K., Lange, J. J. and McKinney, S. A.** (2015). Egr-5 is a post-mitotic
660 regulator of planarian epidermal differentiation. *Elife*.
661 **van Wolfswinkel, J. C., Wagner, D. E. and Reddien, P. W.** (2014). Single-cell analysis reveals functionally
662 distinct classes within the planarian stem cell compartment. *Cell stem cell* **15**, 326-339.
663 **Wagner, D. E., Wang, I. E. and Reddien, P. W.** (2011). Clonogenic neoblasts are pluripotent adult stem
664 cells that underlie planarian regeneration. *Science (New York, N.Y.)* **332**, 811-816.

665 **Wenemoser, D., Lapan, S. W., Wilkinson, A. W., Bell, G. W. and Reddien, P. W.** (2012). A molecular
666 wound response program associated with regeneration initiation in planarians. *Genes & development*
667 **26**, 988-1002.
668 **Wenemoser, D. and Reddien, P. W.** (2010). Planarian regeneration involves distinct stem cell responses
669 to wounds and tissue absence. *Developmental biology* **344**, 979-991.
670 **Witchley, J. N., Mayer, M., Wagner, D. E., Owen, J. H. and Reddien, P. W.** (2013). Muscle cells provide
671 instructions for planarian regeneration. *Cell reports* **4**, 633-641.
672 **Wurtzel, O., Cote, L. E., Poirier, A., Satija, R., Regev, A. and Reddien, P. W.** (2015). A generic and cell-
673 type-specific wound response precedes regeneration in planarians. *Developmental cell* **35**, 632-645.
674 **Zayas, R. M., Cebrià, F., Guo, T., Feng, J. and Newmark, P. A.** (2010). The use of lectins as markers for
675 differentiated secretory cells in planarians. *Developmental dynamics : an official publication of the*
676 *American Association of Anatomists* **239**, 2888-2897.
677 **Zhu, S., Hallows, S. E., Currie, K. W., Xu, C. and Pearson, B. J.** (2015). A mex3 homolog is required for
678 differentiation during planarian stem cell lineage development. *Elife* **4**.

679

680